ESC European Society of Cardiology

European Heart Journal - Cardiovascular Imaging (2022) **23**, 200–208
doi:10.1093/ehjci/jeaa354

Trabecular complexity as an early marker of cardiac involvement in Fabry disease

Antonia Camporeale [1*†], Francesco Moroni[2*†], Davide Lazzeroni[3], Silvia Garibaldi[4], Maurizio Pieroni[5], Federico Pieruzzi[6], Paola Lusardi[7], Marco Spada[8], Renzo Mignani[9], Alessandro Burlina[10], Francesca Carubbi[11], Laura Econimo[12], Yuri Battaglia[13], Francesca Graziani[14], Silvia Pica[1], Kelvin Chow[15], Paolo G. Camici[2], and Massimo Lombardi[1]

[1]Multimodality Cardiac Imaging Section, IRCCS Policlinico San Donato, San Donato Milanese, Via Morandi 30, Milan 20097, Italy; [2]Cardiothoracic and Vascular Department, IRCCS Ospedale San Raffaele and Vita-Salute San Raffaele University, Milan, Italy; [3]Department of Cardiology, IRCCS Don Carlo Gnocchi Foundation, Via Olgettina 60, 20132 Milan, Italy; [4]Department of Cardiology, Parma University Hospital, Parma, Italy; [5]Department of Cardiology, San Donato Hospital, Arezzo, Italy; [6]Nephrology and Dialysis Unit, Department of Medicine and Surgery, University of Milano Bicocca, ASST-Monza San Gerardo Hospital, Monza, Italy; [7]Department of Cardiology, Humanitas Hospital, Torino, Italy; [8]Department of Pediatrics, University of Torino, Torino, Italy; [9]Nephrology and Dialysis Department, Infermi Hospital, Rimini, Italy; [10]Neurological Unit, St. Bassiano Hospital, Bassano del Grappa, Italy; [11]Metabolic Medicine Unit, University of Modena and Reggio Emilia, Modena, Italy; [12]Nephrology and Dialysis Unit, Hospital of Montichiari, Spedali Civili Brescia, Italy; [13]Nephrology and Dialysis Unit, University-Hospital St. Anna, Ferrara, Italy; [14]Department of Cardiovascular and Thoracic Sciences, Fondazione Policlinico Universitario A. Gemelli IRCCS, Rome, Italy; and [15]Cardiovascular MR R&D, Siemens Medical Solutions USA, Inc., Chicago, IL, USA

Received 14 April 2020; editorial decision 10 December 2020; accepted 15 December 2020; online publish-ahead-of-print 22 January 2021

Aims Fabry cardiomyopathy is characterized by glycosphingolipid storage and increased myocardial trabeculation has also been demonstrated. This study aimed to explore by cardiac magnetic resonance whether myocardial trabecular complexity, quantified by endocardial border fractal analysis, tracks phenotype evolution in Fabry cardiomyopathy.

Methods and results Study population included 20 healthy controls (12 males, age 32±9) and 45 Fabry patients divided into three groups: 15 left ventricular hypertrophy (LVH)-negative patients with normal T1 (5 males, age 28±13; Group 1); 15 LVH-negative patients with low T1 (9 males, age 33±9.6; Group 2); 15 LVH-positive patients (11 males, age 53.5±9.6; Group 3). Trabecular fractal dimensions (Dfs) (total, basal, mid-ventricular, and apical) were evaluated on cine images. Total Df was higher in all Fabry groups compared to controls, gradually increasing from controls to Group 3 (1.27±0.02 controls vs. 1.29±0.02 Group 1 vs. 1.30±0.02 Group 2 vs. 1.34±0.02 Group 3; $P<0.001$). Group 3 showed significantly higher values of all Dfs compared to the other Groups. Both basal and total Dfs were significantly higher in Group 1 compared with controls (basal: 1.30±0.03 vs. 1.26±0.04, $P=0.010$; total: 1.29±0.02 vs. 1.27±0.02, $P=0.044$). Total Df showed significant correlations with: (i) T1 value ($r=-0.569$; $P<0.001$); (ii) LV mass ($r=0.664$, $P<0.001$); (iii) trabecular mass ($r=0.676$; $P<0.001$); (iv) Mainz Severity Score Index ($r=0.638$; $P<0.001$).

Conclusion Fabry cardiomyopathy is characterized by a progressive increase in Df of endocardial trabeculae together with shortening of T1 values. Myocardial trabeculation is increased before the presence of detectable sphingolipid storage, thus representing an early sign of cardiac involvement.

Keywords Fabry disease • cardiac magnetic resonance • fractal analysis • T1 mapping

*Corresponding author. Tel: +39 (02) 5277 4804/4376; Fax: +39 (02) 5277 4272 (A.C.). E-mail: antonia.camporeale@grupposandonato.it; Tel: +02 (2643) 6206. E-mail: moroni.francesco@hsr.it (F.M.)
†These authors contributed equally to this work.

Introduction

Fabry disease is a rare X-linked lysosomal disorder caused by an enzymatic deficiency in α-galactosidase A, leading to progressive accumulations of glycosphingolipids (globotriaosylceramide, Gb3) in multiple organs.[1] Specific therapies including enzyme replacement therapy (ERT) and pharmacological chaperones are currently available to prevent, reverse, or slow disease progression.[2–4] Cardiac involvement is characterized by progressive left ventricular hypertrophy (LVH), complicated by myocardial fibrosis and inflammation leading to clinical manifestations including chest pain, arrhythmias, and heart failure,[5] with cardiovascular disease being the main cause of death in these patients.[6] Identification of myocardial fibrosis in advanced stages of the disease by cardiac magnetic resonance (CMR) has been associated with poor response to ERT; therefore, early detection of cardiac involvement is crucial to optimize the therapeutic strategy and improve prognosis.[7]

A disproportionate increase in myocardial trabeculation has been recently described in Fabry cardiomyopathy.[8] Beyond quantification of trabecular mass and its relative contribution as percentage of the overall LV mass, trabecular complexity can be evaluated by fractal analysis of the endocardial border in CMR cine images.[9] Fractal analysis is a method of quantifying complex natural phenomena and biological structures characterized by repetition of self-similar patterns. It has already been used in the study of different aspects of the cardiovascular system, from the complexity of the intracellular structures to heart rate variability.[10] When applied to the indented interface between myocardial wall and LV cavity, fractal analysis can accurately measure the complexity of the endocardial border. The resulting unitless measure index, the fractal dimension (Df), is a non-integer value and it ranges from 1 (simple structure, i.e. straight line) to 2 (complex structure that completely fills the space) when measuring in 2D space; the greater the Df, the more complex the structure is. Fractal analysis has already been used for quantification of trabecular complexity in patients with left ventricular non-compaction, providing higher accuracy and reproducibility compared with the other CMR methods.[11] Beyond a detailed morphological description, CMR with native T1 mapping allows a non-invasive detection of myocardial sphingolipid accumulation resulting in shortening of native T1 values. Low myocardial T1 values have been described in 85% of Fabry disease patients with LVH and ∼50% of Fabry disease patients without LVH.[12] However, it is not clear whether a relationship exists between trabecular complexity and sphingolipid storage in Fabry disease.

This study aimed to understand whether myocardial trabecular complexity, quantified by endocardial border fractal analysis, tracks phenotype evolution in Fabry cardiomyopathy.

Methods

Study population

This observational, retrospective study received approval from the local research ethics committee (Ethical Committee IRCCS San Raffaele Hospital, reference number 135/int/2018), and all participants provided written informed consent. The study population included 45 patients (25 males, mean age 38.0 ± 15.2) with genetically confirmed Fabry disease (Supplementary data online, *Table SA*) referred for CMR at the Multimodality Cardiac Imaging Unit of Policlinico San Donato from December 2015 to December 2018. Patient evaluation included CMR and quantification of global disease burden by Mainz Severity Score Index (MSSI), a specific score of disease severity for Fabry disease.[13] Patients were compared with gender, age, and body surface area (BSA)-matched cohorts of 20 healthy volunteers (12 males, mean age 32.1 ± 9).

The patient population was divided into three groups according to the presence/absence of LVH and low/normal native myocardial T1 values. LVH was defined as an increased LV wall thickness ≥13 mm in one or more LV myocardial segments.[14,15] Reference T1 values in healthy volunteers were used to define low T1 values (>2 SD below mean of healthy controls). The three groups were defined in order to represent three phases of Fabry cardiomyopathy with increasing severity: Group 1, Fabry disease patients with no detectable signs of cardiac involvement (no LVH, normal T1; Group 2) Fabry disease patients with early sphingolipid storage (no LVH, low T1; Group 3) Fabry disease patients with LVH and low T1.

CMR study

CMR was performed on a 1.5 T magnet (MAGNETOM Aera, Siemens Healthcare, Erlangen Germany). Each scan included: (i) retrospectively gated, breath-held, balanced steady-state free-precession cine images (three long-axis views, full LV short-axis stack; slice thickness, 8.0 mm; no gap; flip angle, 60°–80°; repetition time, 3.8 ms; echo time, 1.7 ms; typical readout field of view, 350 mm; phase resolution, 75%; typical acquired voxel size 1.4×1.4 mm; lines per segment, 15); (ii) prototype shortened modified look-locker inversion recovery sequence[16] (ShMOLLI; Work-in-Progress #780B VD13A-SP4; three long-axis views, basal, mid-ventricular, and apical short axis) before and 15 min after 0.1 mmol/kg of contrast (Gadovist, Bayer Schering Pharma, Berlin, Germany) for T1 mapping; and (iii) 2D gradient echo inversion recovery late gadolinium enhancement (LGE) images (three long-axis views, full LV short-axis stack) 8–10 min after contrast.

Non-fractal image analysis

LV volumes, mass, and ejection fraction were calculated from steady-state free-precession cine images and indexed to BSA using a thresholding method on a commercially available software (Qmass, MR version 6.2.1; Medis Medical Imaging Systems, Leiden, The Netherlands). A comprehensive description of the thresholding method is reported in the Supplementary data online. For each myocardial segment, according to the AHA 16 segments model, maximum end-diastolic wall thickness was measured in cine images. Both papillary muscles and trabeculae were included in the computation of global LV mass. To assess compacted LV mass, the endocardial border was drawn to include papillary muscle and exclude LV trabeculation. The trabeculated LV mass was calculated as follows: trabeculated LV mass=global LV mass—compacted LV mass. Trabeculated LV mass was also expressed as a percentage of total LV mass and indexed by BSA.

Anterior mitral leaflet (AML) length was measured in diastole in the three-chambers view, with the leaflets maximally extended parallel to the anterior septum and LV free wall as previously described by Maron *et al.*[17]

The three long-axis views were evaluated for the presence of myocardial crypts, defined as narrow, deep blood-filled invaginations penetrating >50% of the thickness of adjoining myocardium during diastole.[18]

Inline-generated T1 maps were analysed using Argus software (Siemens Healthcare, Erlangen, Germany). T1 values were measured in the interventricular septum and in basal infero-lateral wall, taking care to clearly avoid the blood-myocardial boundary. The classification of

patients according to T1 status (low/normal) was performed considering only septal T1 values (average value between mid-ventricular short axis and horizontal and three-chambers long axis). T1 measurements in basal, mid-ventricular, and apical septum from short-axis views were also reported. Two expert operators (A.C. and S.P., Level 3 EACVI-CMR Certification) performed T1-mapping analyses: A.C. analysed the same T1-mapping sequences twice for intra-observer reproducibility, S.P. reanalysed the same images to assess inter-observer variability.

Fractal analysis of endocardial profile

Fractal analysis of the endocardial profile was performed on end-diastolic frames for each slice of short-axis cine images as previously described, using the open-source image processing software Fiji (Fiji Is Just ImageJ, https://fiji.sc/).[11,19] First, to ensure standardized analysis, the images were automatically thresholded and binarized using a modified version of the IsoData algorithm.[20] The endocardial contour was then extracted from the binarized image using the Sobel operator.[21] A region of interest (ROI) including the left ventricular cavity and the endocardial border was manually traced for each slice. Subsequent analyses were performed on a zoomed image of the ROI. Papillary muscle contours were included in the endocardial border, as previously described.[11] Fractal analysis of the endocardial border was then performed using the standard box-counting method available in the FracLac plug-in (Karperien, A., version 2.5, 1e), as previously described.[19] The resulting output, Df, was a measure of overall contour complexity.

In order to obtain a measure of global and regional endocardial complexity, average Df was obtained for basal, mid-ventricular, and apical segments, and eventually for the entire LV cavity. Myocardial segmentation in basal, mid-ventricular, and apical segments was performed according to the American Heart Association 17 segments model as endorsed by the Society for Cardiovascular Magnetic resonance.[22] In brief, Df of the slices encompassing basal segments was averaged to obtain basal Df, and the process was repeated for mid-ventricular and apical segments. Global LV Df was obtained by averaging Df of all slices. Mean number of slice analysed for each patient was 9.2 ± 1.0 (3.0 ± 0.5 basal, 3.1 ± 0.5 mid-ventricular, and 3.0 ± 0.5 apical). This approach was meant to avoid potential overestimation of trabecular complexity by the use of single slice maximal Df, as well as trying to reduce the influence of potential random error in measurement, which could lead to excessively high, outlier estimation of Df on a single slice.

Myocardial trabecular Df was evaluated by an investigator (F.M.) blinded to relevant clinical and imaging data. F.M. repeated the same analysis twice after 1 month for intra-observer reproducibility. Inter-observer reproducibility was evaluated by two independent rater (A.C. and F.M.), blinded to each other scoring.

Statistical analysis

Continuous variables were expressed as mean (M) and standard deviation (SD), while categorical variables as number (*n*) and percentage (%). The Kolmogorov–Smirnov test was used to assess the normal distribution of data collected. Analysis of variance (ANOVA) and Pearson χ^2 test compared groups for continuous and categorical variables, respectively. *Post hoc* analysis was performed with least significant difference (LSD) test. Pearson's correlation was used to evaluate relationship between continuous variables. Significance was defined as *P*-value <0.05. Intra- and inter-observer reproducibility of Df data were assessed on a subset of 15 randomly selected subjects, for a total of 137 images. Paired Df measures were analysed with Bland–Altman method and intraclass correlation coefficients (ICCs), as well as by calculating repeatability and variation coefficients (COV). All statistics were performed with SPSS version 24 (IBM Corporation).

Results

Study population

Study population included 60 subjects: 20 healthy volunteers (12 males, age 32 ± 9); Group 1: 15 Fabry patients with no detectable signs of cardiac involvement (no LVH, normal T1; 5 males, age 28 ± 13); Group 2: 15 Fabry patients with early sphingolipid storage (no LVH, low T1; 9 males, age 33 ± 9.6); Group 3: 15 Fabry patients with LVH (11 males, age 53 ± 9.6; Group 3). Mean age was 37.5 ± 14.2 and male gender was prevalent (58%); all subjects were Caucasian (all Italians). No differences were found in terms of gender, number of patients with 'classic' mutation, arterial hypertension, and BSA between groups. Age was significantly higher in Group 3. Baseline characteristics of the study populations are further detailed in *Table 1*.

No significant between-group differences in terms of LV end-diastolic volume index (LVEDVi), end-systolic volume index (LVESVi), stroke volume (SV), and LV ventricular ejection fraction (LVEF) were observed.

As expected, index left ventricular mass (LVMass i) progressively increased from the healthy controls to Group 3. Similarly, anterior mitral valve leaflet (AMVL) length and number of crypts as well as trabecular mass (both absolute and indexed value) were progressively higher from control to Group 3, likely reflecting the worsening of the hypertrophic phenotype. The trabecular LV mass expressed as a percentage of total LV mass decreased in Group 3 compared with Group 2 due to the significant increase of total LV mass in these patients. No patients in Group 1 showed LGE, while LGE was detected in two patients (13%) of Group 2 and in 11 patients (73%) of Group 3. Native T1 measurements in Group 1 were within the normal range defined by controls, while T1 values were lower in Group 2. In Group 3, T1 values were low in the septum but a pseudo-normalization of T1 in the infero-lateral wall was found, coincidental with the high frequency of LGE in this location. Considering only septal T1 values, a progressive lowering from controls to Group 3 was observed. A progressive increase from basal-to-apex T1 values was found in all study groups.

Fractal analysis

Total Df was higher in all Fabry groups compared to controls, with total Df gradually increasing from healthy controls to Group 3 (1.27 ± 0.02 in controls vs. 1.29 ± 0.02 in Group 1 vs. 1.30 ± 0.02 in Group 2 vs. 1.34 ± 0.02 in Group 3; $P < 0.001$); *Table 2*; *Figures 1 and 2*. In particular, Group 3 showed significantly higher values of total Df compared to the other Groups, while no significant difference was observed between Groups 1 and 2. A similar trend was observed also when basal, mid-ventricular, and apical Dfs were analysed separately.

Interestingly, both basal and total Dfs of myocardial trabeculae were significantly higher in Group 1 compared with controls (basal: 1.30 ± 0.03 vs. 1.26 ± 0.04, $P = 0.010$; total: 1.29 ± 0.02 vs. 1.27 ± 0.02, $P = 0.044$).

All these differences in Df among the Groups were confirmed and amplified when only patients with 'classic' mutations were considered (Supplementary data online, *Table SB*).

Table 1 Characteristics of study population

	Healthy volunteers ($n = 20$)	Fabry Group 1 LVH−, normal T1 ($n = 15$)	Fabry Group 2 LVH−, low T1 ($n = 15$)	Fabry Group 3 LVH+ ($n = 15$)	*P* value
Demographic data					
Age (years)	32 ± 9	28 ± 13	33 ± 9.6	53 ± 9.6[a]	<0.001*
Male, *n* (%)	12 (60.0)	5 (33.3)	9.0 (60)	11 (73.3)	0.158
BSA (m^2)	1.9 ± 0.22	1.6 ± 0.45	1.76 ± 0.17	1.74 ± 0.23	0.574
'Classic' mutation, *n* (%)	NA	8 (53%)	12 (80%)	11 (73%)	0.260
Arterial hypertension, *n* (%)	0	0	0	2 (13.3)	0.102
CMR data					
LVEF (%)	70.0 ± 4.8	70.3 ± 7.4	69.9 ± 6.7	69.8 ± 8.3	0.985
LVmass i (g/m^2)	58.4 ± 11.6	58.9 ± 8.7	78.3 ± 10.3[a]	144.4 ± 43.9[a]	<0.001*
LVWT (mm)	7.6 ± 0.8	7.5 ± 1.0	10.3 ± 1.2[a]	17.9 ± 3.7[a]	<0.001*
LVEDVi (mL/m^2)	73.2 ± 13.3	72.9 ± 12.7	78.5 ± 14.1	68.7 ± 14.7	0.274
LVESVi (mL/m^2)	22.3 ± 5.8	22.2 ± 7.1	23.87 ± 8.7	19.9 ± 6.7	0.486
SV (mL)	92.4 ± 22.2	88.4 ± 11.5	96.1 ± 16.2	86.0 ± 21.8	0.421
Trabecular mass (g)	17.4 ± 5.6	23.8 ± 6.5	33.2 ± 8.7[a]	64.1 ± 34.7[a]	<0.001*
Trabecular mass (%)	15.9 ± 2.1	20.4 ± 2.9[a]	22.5 ± 3.4[a]	21.1 ± 3.2[a]	<0.001*
Trabecular mass index (g/m^2)	9.7 ± 2.3	13.8 ± 5.3	18.9 ± 4.2[a]	36.3 ± 18.4[a]	<0.001*
AMVL (mm)	21.6 ± 2.5	22.47 ± 3.0	24.7 ± 2.9[a]	29.5 ± 6.2[a]	<0.001*
Crypts, *n* (%)	1 (0)	2 (13)	2 (13)	5 (33)	0.141
LGE positive, *n* (%)	0 (0)	0 (0)	2 (13)	11 (78)	<0.001*
LGE n° segments, *n*	0 (0)	0 (0)	2 (1)	27 (11)	<0.001*
Septal T1 (ms)	965 ± 19	965 ± 21	843 ± 47[a]	838 ± 52[a]	<0.001*
Basal septal T1 (ms)	961 ± 22	951 ± 34	848 ± 42[a]	823 ± 59[a]	<0.001*
Mid septal T1, ms	968 ± 34	962 ± 29	852 ± 50[a]	851 ± 54[a]	<0.001*
Apical septal T1 (ms)	980 ± 54	987 ± 48	873 ± 66[a]	882 ± 64[a]	<0.001*
Infero-lateral T1 (ms)	949 ± 38	937 ± 48	846 ± 51[a]	926 ± 92	<0.001*
MSSI	0 ± 0	7.5 ± 5.1 ‡	15.9 ± 9.0[a]	28.6 ± 11.8[a]	<0.001*

Data are presented as mean ± SD or *n* (%).
AMVL, anterior mitral valve leaflet; BSA, body surface area; LGE, late gadolinium enhancement; LVEDV i, left ventricular end-diastolic volume index to BSA; LVEF, left ventricular ejection fraction; LVESV i, left ventricular end-systolic volume index to BSA; LVH, left ventricular hypertrophy; LVMass i, left ventricular mass indexed to BSA; LVWT, maximum left ventricular wall thickness; MSSI, Mainz Severity Score Index; SV, stroke volume.
[a]*Post hoc* LSD correction ($P < 0.05$) comparing each Fabry group with controls.
*$P < 0.05$ considered as statistically significant.

Table 2 Fractal dimensions in different stages of Fabry cardiomyopathy and healthy controls

	Healthy volunteers ($n = 20$)	Fabry Group 1 LVH−, normal T1 ($n = 15$)	Fabry Group 2 LVH−, low T1 ($n = 15$)	Fabry Group 3 LVH+ ($n = 15$)	*P* value
Total Df	1.27 ± 0.02	1.29 ± 0.02[a]	1.30 ± 0.02[a]	1.34 ± 0.02[a]	<0.001*
Basal Df	1.26 ± 0.04	1.30 ± 0.03[a]	1.29 ± 0.05[a]	1.34 ± 0.04[a]	<0.001*
Mid-ventricular Df	1.31 ± 0.03	1.31 ± 0.03	1.33 ± 0.03	1.37 ± 0.03[a]	<0.001*
Apical Df	1.23 ± 0.05	1.25 ± 0.05	1.28 ± 0.05[a]	1.32 ± 0.05[a]	<0.001*

Data are presented as mean ± SD.
Df, fractal dimension.
[a]Post hoc LSD correction ($P < 0.05$) comparing each Fabry group with controls.
*$P < 0.05$ considered as statistically significant.

Due to the inclusion of papillary muscles in the fractal analysis, mid-ventricular Df was greater than basal and apical Df in all groups. Hypertrophy of papillary muscles has been previously described in Fabry cardiomyopathy.[23]

For the combined population of all Fabry patients, total Df showed significant correlations with: (i) MSSI ($r = 0.638$; $P < 0.001$); (ii) LV mass ($r = 0.664$, $P < 0.001$); (iii) maximum left ventricular wall thickness (LVWT) ($r = 0.703$; $P < 0.001$); (iv) trabecular mass ($r = 0.676$;

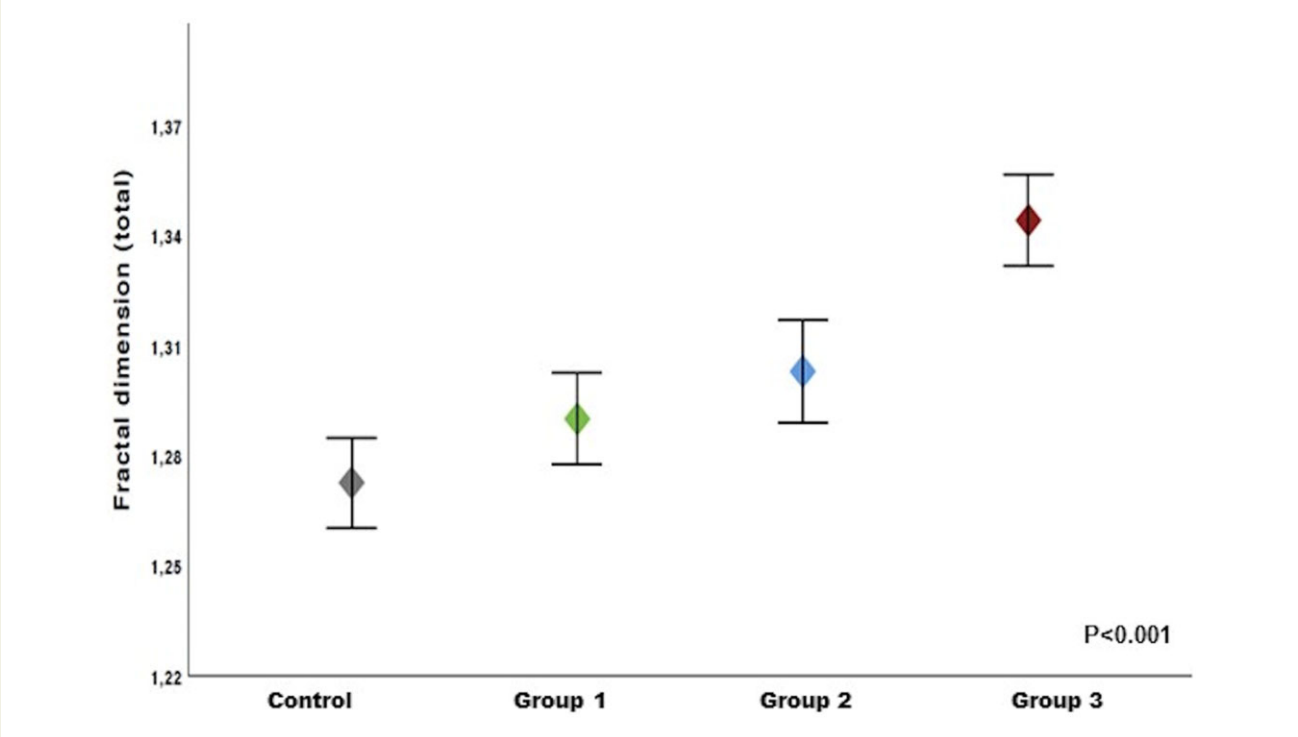

Figure 1 Total myocardial trabecular complexity (mean and standard error 95% values) quantified by endocardial border fractal analysis in different stages of Fabry cardiomyopathy and healthy controls. *P* value refers to ANOVA test comparing all Groups.

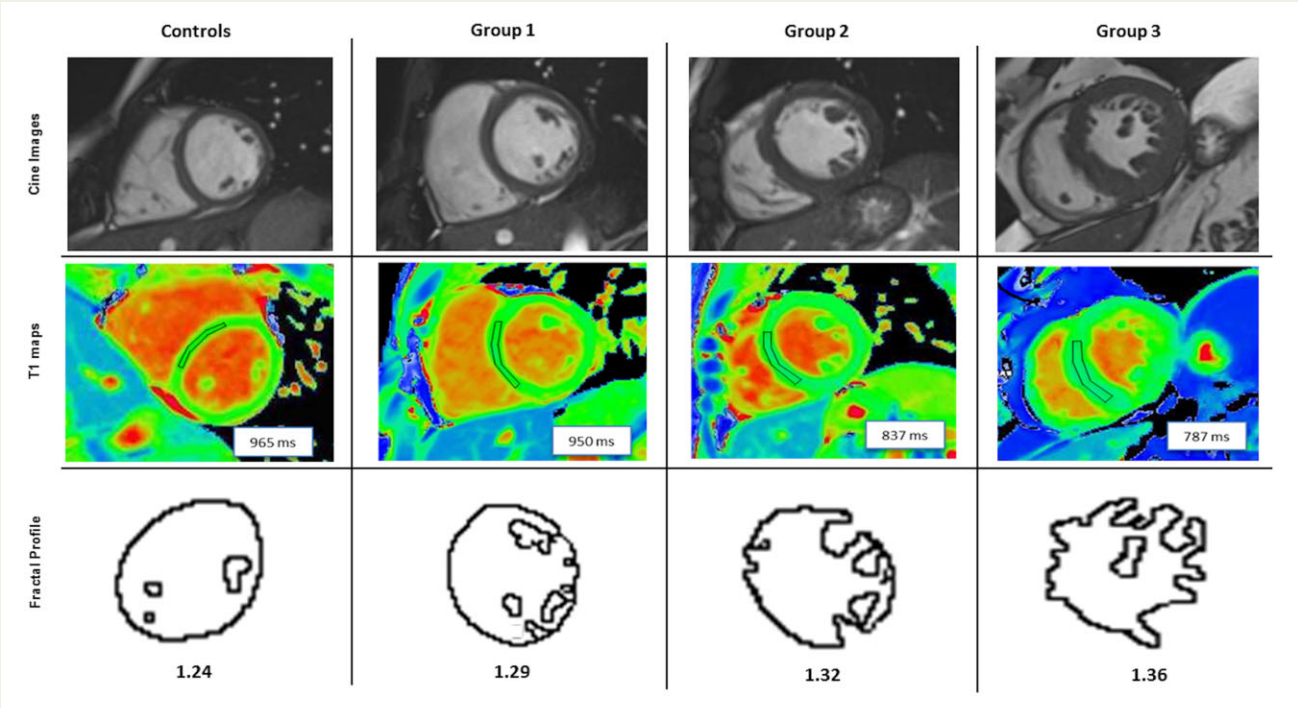

Figure 2 Cine images (upper panels), T1 maps (middle panels), and trabecular fractal dimension (lower panels) showing a mid-LV short-axis slice of four subjects, one from each groups. Moving from controls to Group 3 (left to right), progressive increase in fractal dimension together with lowering of T1 values, and increase of LV mass can be observed. Patient from Group 1 without any detectable sign of cardiac involvement (normal T1 value and no LVH) shows a greater trabecular complexity compared to control, thus suggesting that increased myocardial trabeculation can be a very early sign of cardiac involvement in Fabry Disease. LVH, left ventricular hypertrophy.

Table 3 Correlations of total fractal dimension with CMR and clinical parameters

	Correlation coefficient	*P*-value
Age	0.493	<0.001*
MSSI	0.638	<0.001*
LV mass i (g/m^2)	0.664	<0.001*
Trabecular mass (g)	0.676	<0.001*
Trabecular mass (%)	0.593	<0.001*
Trab. Mass Index (g/m^2)	0.769	<0.001*
LVWT (mm)	0.703	<0.001*
Septal T1 (ms)	-0.569	<0.001*
Basal septal T1 (ms)	-0.599	<0.001*
Mid septal T1 (ms)	-0.489	<0.001*
Apical septal T1 (ms)	-0.338	0.009
Infero-lateral T1 (ms)	-0.108	0.410

LV mass i, left ventricular mass indexed to BSA; LVWT, maximum left ventricular wall thickness; MSSI, Mainz Severity Score Index.
*$P < 0.05$ considered as statistically significant.

$P < 0.001$); and (v) septal T1 values ($r = -0.569$; $P < 0.001$); *Table 3* and *Figure 3*.

Reproducibility analysis

Fractal analysis showed a good intra- and inter-observer reproducibility, with no bias evident on the Bland–Altman plot (Supplementary data online, *Figure SA* and *SB*). ICC for intra-observer reproducibility showed a satisfactory correlation between repeated measures (ICC=0.87, 95% CI: 0.83–0.91, $P < 0.0001$). The coefficient of repeatability was 0.077, while the COV was 2.1%. For inter-observer reproducibility ICC was 0.92 (95% CI: 0.89–0.94, $P < 0.001$), COV 1.6% and coefficient of repeatability 0.057.

Native myocardial T1 measurements with ShMOLLI were highly reproducible. Intra-observer and inter-observer reproducibilities were similarly good, showing an ICC of 0.99 and a COV of 7.58% for intra-observer reproducibility and 7.88% inter-observer reproducibility.

Discussion

Early detection of organ damage represents a major challenge in the clinical management of Fabry disease with significant therapeutic and prognostic implications.[24] In recent years, CMR has emerged as an important technique to identify subclinical cardiac involvement with early detection of glycosphingolipid storage by T1 mapping. We recently showed that low T1 values in LVH negative Fabry patients are associated with early morphological and ECG changes and predict disease progression at 1-year follow-up.[25]

This study demonstrates that myocardial trabeculation progressively increases together with the development of Fabry cardiomyopathy and that increased trabecular complexity, measured by fractal analysis, precedes LVH and T1 shortening, thus representing an earlier sign of cardiac involvement. In this study, both basal and total Dfs were significantly higher in Fabry patients compared to controls, even in the subgroup without any detectable sign of cardiac involvement with T1. Moreover, we demonstrated that trabecular complexity parallels the evolution of cardiac phenotype of Fabry disease with a progressive increase in more advanced stages characterized by increase of LV mass and lowering of native myocardial T1 values. The quantification of trabecular mass (both as absolute value and indexed by BSA) in addition to the measurement of trabecular complexity by fractal dimension reinforced these concepts. However, the quantification of trabecular mass and the fractal analysis of endocardial border do not express the same concept: the same mass of myocardial trabeculae can generate different degree of complexity (and, consequently, of fractal dimension) according to its spatial distribution. Thus, these concepts are complementary rather than alternative. Nevertheless, fractal analysis has previously shown greater reproducibility compared to other measurements[11] and allowed a regional quantification of trabecular complexity in basal, mid-ventricular, and apical LV segments, thus adding further information about LV morphology.

The presence of significantly increased Df in Fabry population compared with controls reinforces the concept that increased myocardial trabeculation represents an early morphological feature of Fabry cardiomyopathy, even if not specific for this disease. Increased myocardial trabecular complexity has been described, together with elongation of anterior mitral valve leaflets and high frequency of crypts, as one of the preclinical abnormalities in hypertrophic cardiomyopathy (HCM) gene mutation carriers without LVH.[26] In HCM, the presence of the mutation and the consequent sarcomere defect have been considered sufficient *per se* to determine these morphological alterations independently of LVH, although the mechanisms have not been clarified. Similarly, in Fabry cardiomyopathy increased myocardial trabeculation occurs before the development of a significant LVH and before significant myocardial glycosphingolipids storage as detectable by T1 mapping has occurred. This study confirms and expands the recent observations by Nordin *et al.*[9] reporting a higher maximal apical Df and longer anterior mitral valve leaflets in a subset of Fabry patients without LVH compared with healthy volunteers. In their study, the detection of increased myocardial trabeculation even in the absence of a significant T1 lowering led the authors to consider these early morphological alterations as 'storage-independent'. Nevertheless, in our study, the evaluation of patients with different stages of cardiac involvement allowed to demonstrate a progressive increase of trabecular complexity in patients with LVH and in later stages of Fabry cardiomyopathy, together with an inverse linear correlation between fractal dimension and T1 values. These findings suggest that myocardial trabeculation reflects myocardial glycosphingolipids storage even in the presence of an early myocardial involvement with an initial glycosphingolipid accumulation not yet detectable by current CMR techniques. In fact, although currently representing the only non-invasive tool to detect myocardial storage, the sensitivity, and specificity of T1 mapping have never been evaluated in comparison with histological findings, with no evidence supporting the absence of myocardial storage in patients with Fabry disease and normal T1 values. On the other hand, it is well established by pathology studies that glycosphingolipid storage starts during foetal development, particularly in male patients with classic disease.[27,28] In addition, glycosphingolipid storage has been histologically documented in other target organ tissues like the kidney and the

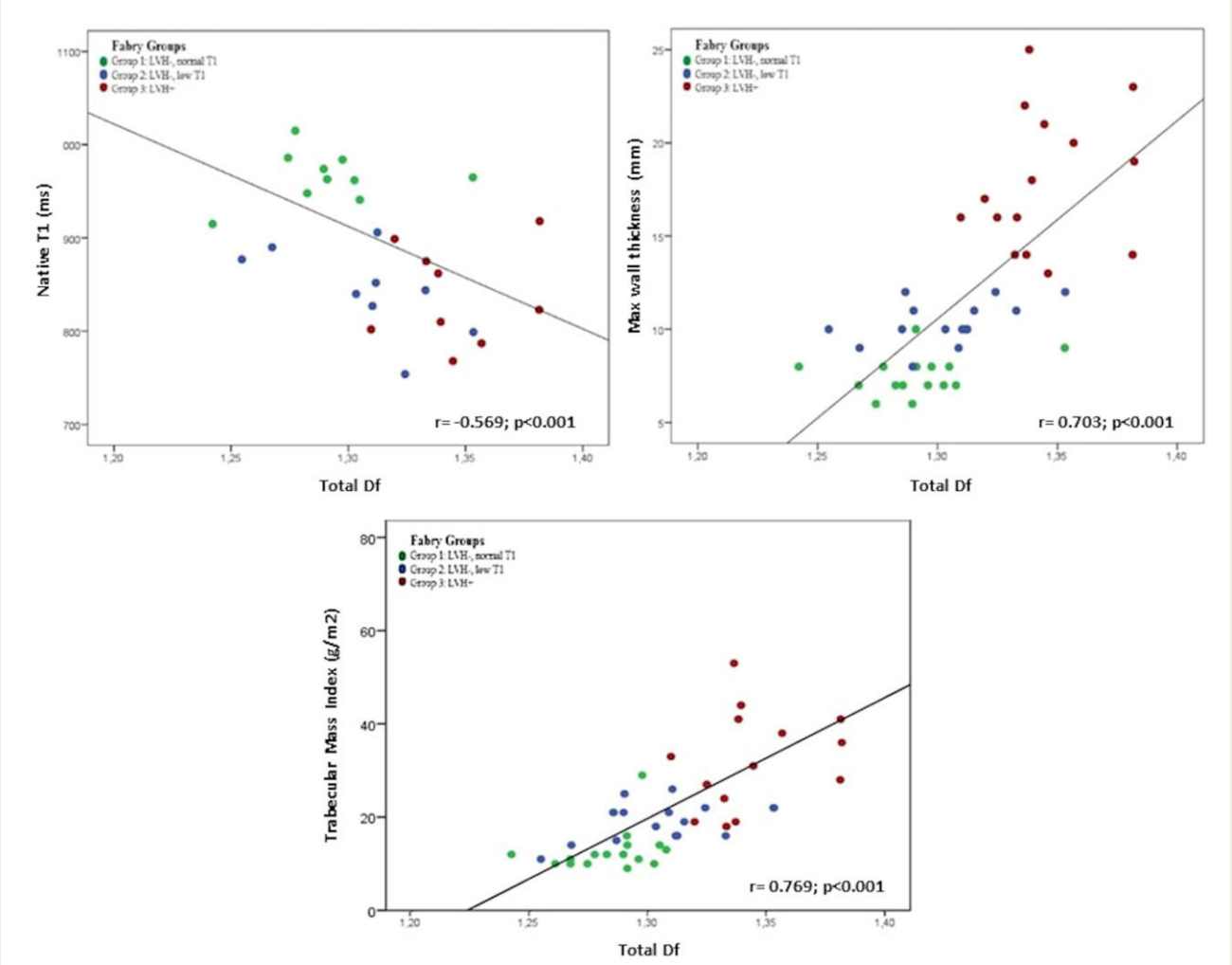

Figure 3 Correlation between total fractal dimension and septal T1 values (*A*), maximum LV wall thickness (*B*), and trabecular mass indexed for BSA (*C*). Df, fractal dimension.

cornea, in children without significant functional alterations.[29] It seems therefore very likely that patients without LVH but with myocardial trabeculation harbour an initial myocardial glycosphingolipid storage. This hypothesis is further supported by the evidence of more pronounced differences in Df between healthy controls and LVH negative patients with normal T1 values when considering only Fabry patients with 'classic' mutation, by definition presenting early storage in target organ tissues.

Concerning the possible mechanisms associating increased trabeculation in Fabry disease with myocardial glycosphingolipid storage, it has been previously demonstrated the presence of an endocardial-epicardial gradient of myocardial storage with an endomyocardial glycosphingolipid compartmentalization characterized by a thickened and glycolipid-engulfed endocardium and a subendocardial severely affected myocardium.[30] It is, therefore, tempting to speculate that early myocardial storage, primarily affecting subendocardial layers, may first manifest as myocardial trabeculation and only when increasing and involving outer myocardial layers as low myocardial T1 signal. However, the measurement of myocardial T1 value in the trabeculated endocardial layer is technically hindered by the complex interface between myocardium and blood. A reliable measurement of T1 can only be obtained by avoiding the blood-myocardial boundary, thus restricting the analysis to the mid-myocardium where storage likely occurs later.

In vitro studies suggest that the presence of a growth-promoting factor leading to a significant proliferative response of cardiomyocytes and vascular smooth muscle cells in Fabry patients with evidence of LVH and an increased intima-media thickness of common carotid artery in the absence of hypertension.[31] We can hypothesize that both in Fabry disease and HCM, beyond a different initial trigger represented by glycosphingolipid storage and abnormal sarcomere protein function, respectively, secondary common pathways are activated, leading initially to increase trabeculation and later to overt LVH. In this view, increased trabeculation should be regarded as the first sign of an initial intrinsic myocardial impairment stimulated by early myocardial tissue abnormalities not yet manifesting as LVH.

Clinical implications

Taken together, our findings suggest that increased myocardial trabeculation may reflect early endomyocardial glycosphingolipid storage and therefore represent a very early marker of cardiac involvement in Fabry disease. If confirmed in larger series, this marker could be useful for early identification of myocardial involvement and consequently to define the better therapeutic approach. There is accumulating evidence that appropriate treatment with both specific and conventional cardiological therapies may affect the disease course and prognosis, with better results when these therapies are promptly initiated.[24]

Limitations of the study

CMR findings were not compared with myocardial histology, so the presence of early sphingolipid storage in Fabry patients with normal T1 values and increased fractal dimension could not be directly confirmed. We cannot exclude that normal T1 values in patients with increased trabeculation and no LVH may be a consequence of current technical limitations limiting T1 measurements to the mid-myocardium due to the complex interface between myocardium and blood.

Conclusions

Cardiac involvement in Fabry disease is characterized by a progressive increase in fractal dimension of endocardial trabeculae. Total myocardial trabeculation is increased in Fabry patients even before the presence of low myocardial T1 values and before the development of LVH, thus representing a very early sign of cardiac involvement.

Supplementary data

Supplementary data are available at *European Heart Journal - Cardiovascular Imaging* online.

Funding

This study was partially supported by Ricerca Corrente funding from Italian Ministry of Health to IRCCS Policlinico San Donato.

Conflict of interest: A.C.: Honoraria for presentations and board meetings from Amicus Therapeutics, Sanofi-Genzyme, and Shire. Research grant from Amicus Therapeutics. M.P.: speaker and advisory board honoraria, and travel support from Sanofi-Genzyme, Amicus Therapeutics, and Shire. F.P.: honoraria from Sanofi-Genzyme, Shire, and Amicus Therapeutics. M.S.: honoraria for speaking fees for symposia and meetings and for advisory board attendance from Sanofi Genzyme and Shire International. R.M.: honoraria and expert witness with Sanofi-Genzyme and Amicus Therapeutics. A.B.: honoraria for presentations and board meetings from Amicus Therapeutics and Sanofi Genzyme. Member of the European Advisory Board of the Fabry Registry, sponsored by Genzyme. F.C.: travel reimbursement, lectures, and advisory boards honoraria from: Sanofi, Shire, Amicus, Amgen, and Mylan. F.G.: travel sponsor from Genzyme, Shire, and Amicus, honoraria speaker for Shire and Genzyme. K.C.: full-time employee of Siemens Medical Solutions USA, Inc. P.G.C.: consultant for Servier.

References

1. Desnick RJ, Ioannou YA, Eng CM. 150: α-galactosidase A deficiency: Fabry disease. In: Lewis A. Barness, *The Metabolic and Molecular Bases of Inherited Disease*, 7th ed. New York, NY: McGraw-Hill, 2001. p3733–74.
2. Eng CM, Guffon N, Wilcox WR, Germain DP, Lee P, Waldek S *et al.*; International Collaborative Fabry Disease Study Group. Safety and efficacy of recombinant human alpha-galactosidase A replacement therapy in Fabry's disease. *N Engl J Med* 2001;**345**:9–16.
3. Schiffmann R, Kopp JB, Austin HA 3rd, Sabnis S, Moore DF, Weibel T *et al.* Enzyme replacement therapy in Fabry disease: a randomized controlled trial. *JAMA* 2001;**285**:2743–9.
4. Germain DP, Hughes DA, Nicholls K, Bichet DG, Giugliani R, Wilcox WR *et al.* Treatment of Fabry's disease with the pharmacologic chaperone migalastat. *N Engl J Med* 2016;**375**:545–55.
5. Linhart A, Elliott PM. The heart in Anderson-Fabry disease and other lysosomal storage disorders. *Heart* 2007;**93**:528–35.
6. Baig S, Edward NC, Kotecha D, Liu B, Nordin S, Kozor R *et al.* Ventricular arrhythmia and sudden cardiac death in Fabry disease: a systematic review of risk factors in clinical practice. *Europace* 2018;**20**:f153–61.
7. Wanner C, Arad M, Baron R, Burlina A, Elliott PM, Feldt-Rasmussen U *et al.* European expert consensus statement on therapeutic goals in Fabry disease. *Mol Genet Metab* 2018;**124**:189–203.
8. Kozor R, Callaghan F, Tchan M, Hamilton-Craig C, Figtree GA, Grieve SM. A disproportionate contribution of papillary muscles and trabeculations to total left ventricular mass makes choice of cardiovascular magnetic resonance analysis technique critical in Fabry disease. *J Cardiovasc Magn Reson* 2015;**17**:22.
9. Nordin S, Kozor R, Baig S, Abdel-Gadir A, Medina-Menacho K, Rosmini S *et al.* Cardiac phenotype of prehypertrophic Fabry disease. *Circ Cardiovasc Imaging* 2018;**11**:e007168.
10. Captur G, Karperien AL, Hughes AD, Francis DP, Moon JC. The fractal heart—embracing mathematics in the cardiology clinic. *Nat Rev Cardiol* 2017;**14**:56–64.
11. Captur G, Muthurangu V, Cook C, Flett AS, Wilson R, Barison A *et al.* Quantification of left ventricular trabeculae using fractal analysis. *J Cardiovasc Magn Reson* 2013;**15**:36.
12. Pica S, Sado D, Maestrini V, Fontana M, White SK, Treibel T *et al.* Reproducibility of native myocardial T1 mapping in the assessment of Fabry disease and its role in early detection of cardiac involvement by cardiovascular magnetic resonance. *J Cardiovasc Magn Reson* 2014;**16**:99.
13. Whybra C, Kampmann C, Krummenauer F, Ries M, Mengel E, Miebach E *et al.* The Mainz Severity Score Index: a new instrument for quantifying the Anderson–Fabry disease phenotype, and the response of patients to enzyme replacement therapy. *Clin Genet* 2004;**65**:299–307.
14. Militaru S, Ginghin C, Popescu BA, Saftoiu A, Linhart A, Jurcut R. Multimodality imaging in Fabry cardiomyopathy: from early diagnosis to therapeutic targets. *Eur Heart J Cardiovasc Imaging* 2018;**19**:1313–22.
15. Yousef Z, Elliott PM, Cecchi F, Escoubet B, Linhart A, Monserrat L *et al.* Left ventricular hypertrophy in Fabry disease: a practical approach to diagnosis. *Eur Heart J* 2013;**34**:802–8.
16. Piechnik SK, Ferreira VM, Dall'Armellina E, Cochlin LE, Greiser A, Neubauer S *et al.* Shortened Modified Look-Locker Inversion recovery (ShMOLLI) for clinical myocardial T1-mapping at 1.5 and 3 T within a 9 heartbeat breathhold. *J Cardiovasc Magn Reson* 2010;**12**:69.
17. Maron MS, Olivotto I, Harrigan C, Appelbaum E, Gibson CM, Lesser JR *et al.* Mitral valve abnormalities identified by cardiovascular magnetic resonance represent a primary phenotypic expression of hypertrophic cardiomyopathy. *Circulation* 2011;**124**:40–7.
18. Captur G, Lopes LR, Mohun TJ, Patel V, Li C, Bassett P *et al.* Prediction of sarcomere mutations in subclinical hypertrophic cardiomyopathy. *Circ Cardiovasc Imaging* 2014;**7**:863–71.
19. Moroni F, Magnoni M, Vergani V, Ammirati E, Camici PG. Fractal analysis of plaque border, a novel method for the quantification of atherosclerotic plaque contour irregularity, is associated with pro-atherogenic plasma lipid profile in subjects with non-obstructive carotid stenoses. *PLoS One* 2018;**13**:e0192600.
20. Ridler T, Calvard S. Picture thresholding using an iterative selection method. *IEEE Trans Syst MAN Cybern* 1978;SMC-8:630–2.
21. Ahammer H, DeVaney TTJ. The influence of edge detection algorithms on the estimation of the fractal dimension of binary digital images. *Chaos* 2004;**14**:183–8.
22. Schulz-Menger J, Bluemke DA, Bremerich J, Flamm SD, Fogel MA, Friedrich MG *et al.* Standardized image interpretation and post processing in cardiovascular magnetic resonance: Society for Cardiovascular Magnetic Resonance (SCMR) board of trustees task force on standardized post processing. *J Cardiovasc Magn Reson* 2013;**15**:35.

23. Kozor R, Nordin S, Treibel TA, Rosmini S, Castelletti S, Fontana M *et al.* Insight into hypertrophied hearts: a cardiovascular magnetic resonance study of papillary muscle mass and T1 mapping. *Eur Heart J Cardiovasc Imaging* 2017;**18**:1034–40.
24. Germain DP, Charrow J, Desnick RJ, Guffon N, Kempf J, Lachmann RH *et al.* Ten-year outcome of enzyme replacement therapy with Agalsidase beta in patients with Fabry disease. *J Med Genet* 2015;**52**:353–8.
25. Camporeale A, Pieroni M, Pieruzzi F, Lusardi P, Pica S, Spada M *et al.* Predictors of clinical evolution in prehypertrophic Fabry disease. *Circ Cardiovasc Imaging* 2019;**12**:e008424.
26. Captur G, Lopes LR, Patel V, Li C, Bassett P, Syrris P *et al.* Abnormal cardiac formation in hypertrophic cardiomyopathy fractal analysis of trabeculae and preclinical gene expression. *Circ Cardiovasc Genet* 2014;**7**:241–8.
27. Kleijer WJ, Iiussaarts-Odijk LM, Sachs ES, Jahoda MGJ, Niermeijer MF. Prenatal diagnosis of Fabry's disease by direct analysis of chorionic villi. *Prenat Diagn* 1987;**7**:283–7.
28. Vedder AC, Strijland A, Vd Bergh Weerman MA, Florquin S, Aerts JM, Hollak CE. Manifestations of Fabry disease in placental tissue. *J Inherit Metab Dis* 2006;**29**:106–11.
29. Tøndel C, Bostad L, Hirth A, Svarstad E. Renal biopsy findings in children and adolescents with Fabry disease and minimal albuminuria. *Am J Kidney Dis* 2008;**51**:767–76.
30. Pieroni M, Chimenti C, De Cobelli F, Morgante E, Del Maschio A, Gaudio C *et al.* Fabry's disease cardiomyopathy: echocardiographic detection of endomyocardial glycosphingolipid compartmentalization. *J Am Coll Cardiol* 2006;**47**:1663–71.
31. Barbey F, Brakch N, Linhart A, Rosenblatt-Velin N, Jeanrenaud X, Qanadli S *et al.* Cardiac and vascular hypertrophy in Fabry disease: evidence for a new mechanism independent of blood pressure and glycosphingolipid deposition. *Arterioscler Thromb Vasc Biol* 2006;**26**:839–44.